

# Computational Fluid Dynamics Analysis of a Maglev Centrifugal Left Ventricular Assist Device

\*†Greg W. Burgreen, ‡Howard M. Loree II, ‡Kevin Bourque, ‡Charles Dague, ‡Victor L. Poirier, ‡David Farrar, \*Edward Hampton, §Z. Jon Wu, ¶Thomas M. Gempp, and ¶¶Reto Schöb

\**Engineering Applied Sciences Inc, Export, PA; †Mississippi State University, Starkville, MS; ‡Thoratec Corp, Pleasanton, CA; §University of Pittsburgh, Pittsburgh, PA, U.S.A.; ¶Levitronix GmbH, Zürich, Switzerland*

---

**Abstract:** The fluid dynamics of the Thoratec HeartMate III (Thoratec Corp., Pleasanton, CA, U.S.A.) left ventricular assist device are analyzed over a range of physiological operating conditions. The HeartMate III is a centrifugal flow pump with a magnetically suspended rotor. The complete pump was analyzed using computational fluid dynamics (CFD) analysis and experimental particle imaging flow visualization (PIFV). A comparison of CFD predictions to

experimental imaging shows good agreement. Both CFD and experimental PIFV confirmed well-behaved flow fields in the main components of the HeartMate III pump: inlet, volute, and outlet. The HeartMate III is shown to exhibit clean flow features and good surface washing across its entire operating range. **Key Words:** Left ventricular assist device—Computational fluid dynamics—Centrifugal flow—Magnetically suspended rotor.

---

## INTRODUCTION

The HeartMate III (Thoratec Corp., Pleasanton, CA, U.S.A.) is an implantable left ventricular assist device (LVAD) designed for long-term use. The pump components of the HeartMate III were originally designed using empiric methods, namely, in vitro testing of multiple configurations using rapid prototyping fabrication techniques (1). The final hydrodynamic configuration of the HeartMate III consists of a low aspect, flattened inflow channel with a 90-degree rounded elbow, a centrally open rotor with shrouded impeller and backswept blading, a constantly increasing area volute with a large radius cutwater, and rather large gaps separating the rotor from the pump housing (Fig. 1). This combination of components was determined to result in minimal thrombogenesis via extensive in vivo calf experimentation (2).

Pumps with magnetically suspended rotors inevitably have multiple internal flow paths. Typically, the main flow path contains pump elements that generate the primary pressure head and fluid flow, and secondary flow paths exist solely to physically separate rotating electromagnetic components from stationary ones. However, all secondary flow paths induce fluid flow usually involving low volumetric flow rates and high shear stresses. The challenge for maglev pumps is to design secondary flow paths such that the key performance metrics of the pump are not compromised beyond utility. The HeartMate III has a rather unusual design in that it has three flow paths: one main flow path and two secondary flow paths. Moreover, one of the secondary flow paths is designed to have an unusually large gap. This is not an intuitive design feature because a large gap secondary flow path is expected to produce excessive flow leakage and severely decrease the pump's hydraulic efficiency.

The primary performance metrics for blood pumps designed for long-term use include low thrombogenesis and adequate hydrodynamic efficiency across all expected operating points. Given the unique geometric features of the HeartMate III and the fact that this pump performs exceptionally well, both in

---

Received March 2004.

Address correspondence and reprint requests to Dr. Greg W. Burgreen, Box 9627, Mississippi State, MS 39762, U.S.A. E-mail: burgreen@erc.msstate.edu

Presented at the 11<sup>th</sup> Congress of the International Society for Rotary Blood Pumps, held August 31–September 2, 2003, in Bad Oeynhausen, Germany.

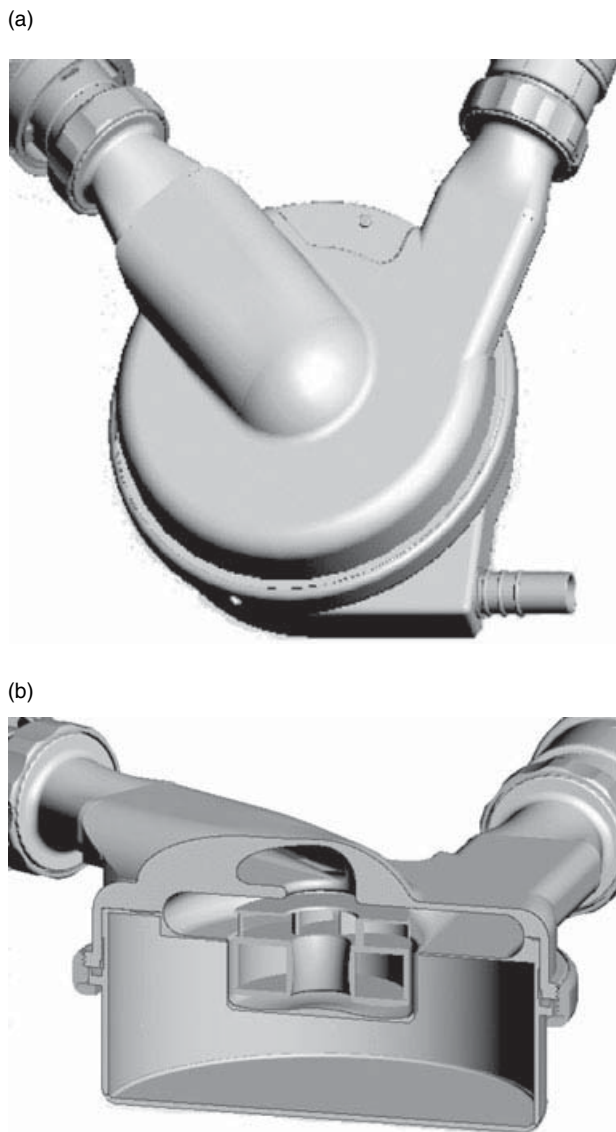


**FIG. 1.** Solid model of the HeartMate III pump: (a) overall view; (b) cross-sectional view.

vitro and in vivo efforts were undertaken to investigate its fluid dynamics in detail. This article reports the findings of complementary computational and experimental studies to characterize flows within the HeartMate III under a range of physiologic conditions.

### METHODS OF ANALYSIS

Computational fluid dynamics (CFD) and laser-based flow visualization were used to analyze the fluid dynamics of the HeartMate III blood pump. Additional details of these two methods of analysis are described below.

### Details of the CFD analysis

The CFD geometry model was created using Initial Graphics Exchange Specification (IGES) surfaces extracted from a CAD model (SolidWorks Corp., Concord, MA, U.S.A.) of the pump. The main flow path of the HeartMate III consists of the inlet channel and its elbow, the centralized opening in the impeller shroud, the blade-to-blade passages, the volute, and the outlet channel. Two secondary flow paths exist. The first such path comprises the small gap passage existing between the outer rotor walls and the lower housing cavity walls, and also includes the central material void of the rotor. The other secondary flow path consists of the large gap between the top surface of the impeller shroud and the upper housing wall. In the clinical version of the pump, all stationary blood-contacting surfaces are finished with a bonded textured (sintered titanium) coating, whereas the rotor is finished with smooth, polished surfaces. The CAD geometry model did not account for the nominal 0.007-inch thickness of the textured coating. From a flow analysis standpoint, this minor thickness still significantly modified the smallest gap widths in the lower housing secondary flow path. Hence, the lower housing cavity surfaces were offset by an appropriate thickness. An unstructured CFD mesh was generated for the pump assembly including all of its components and flow paths. The mesh consisted of 325K nodes and 1.4M tetrahedral cells (Fig. 2).

A finite-volume, unstructured mesh CFD approach was used to solve the unsteady incompressible laminar Navier–Stokes equations using Fluent 6.0 (Fluent Inc., Lebanon, NH, U.S.A.). Because of the high shear rates in the pump, a Newtonian constitutive model could be used. The laminar viscosity was chosen as the asymptotic value for human blood (3.2 Pa·s). Blood density was modeled with a nominal value of 1050 kg/m<sup>3</sup>. The rotational motion of the rotor was explicitly simulated using a sliding mesh interface to couple the rotating domain to the stationary domains. The selected time step size corresponded to the division of one full rotational period into 200 uniform increments. While the simulation was modeled as unsteady to accurately account for rotor–stator interactions, the inflow conditions were assumed to be steady and fixed. This avoids the expenses associated with computing a full cardiac cycle time accurately. CFD analyses were performed at low (3 L/min, 3500 rpm), normal (7 L/min, 4500 rpm), and high (10 L/min, 5200 rpm) operating conditions, representing the full range of expected operating points for the HeartMate III.

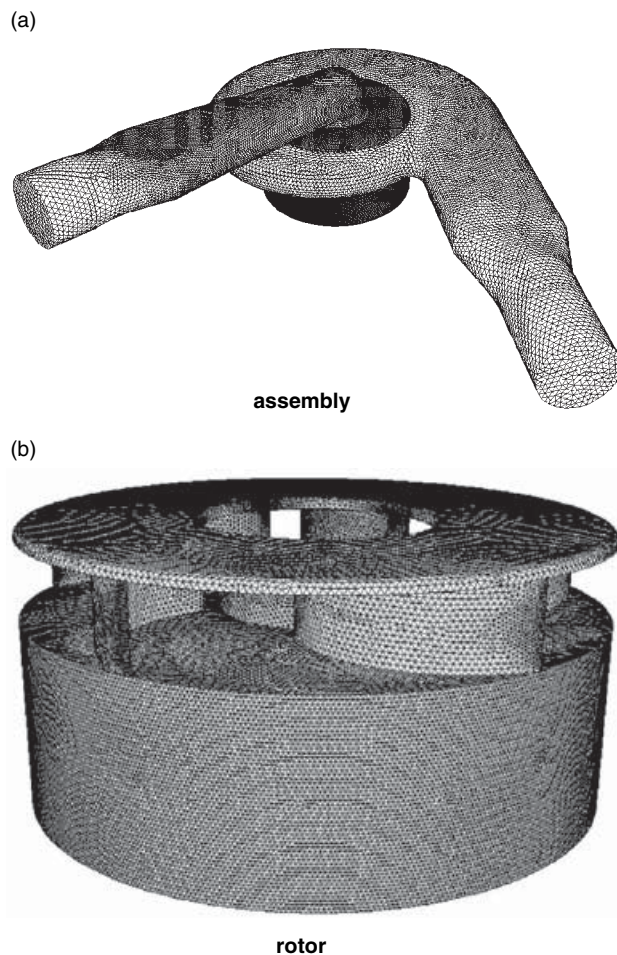


**FIG. 2.** Unstructured mesh of complete pump assembly including centrally open rotor/impeller.

### Details of the flow visualization analysis

Apart from the transparent material and construction of the pump housing, the particle imaging flow visualization (PIFV) analyzed a pump identical to the clinical version including full magnetic levitation, rotor motive action, and electronic control. During pump operation, a sheet of argon laser light excited 30-micron diameter polystyrene fluorescent particles suspended in a blood analog fluid having a density of  $1000 \text{ kg/m}^3$  and a viscosity of  $3.6 \text{ Pa}\cdot\text{s}$ . Using a digital CCD camera (Eastman Kodak Megaplug 1.4, Rochester, NY, U.S.A.), still frame and video images were captured corresponding to a map of streaklines formed by fluid traversing the photographic field of view. Because of the presence of obstructive electromagnetic components, flow visualization was restricted to the inlet flow channel, the volute, and the outlet flow channel. PIFV was used to examine the pump at 13 different viewing planes and 12 different operating conditions ranging from 1 to

12 L/min and 3500 to 5200 rpm. Hydraulic (H-Q) testing was also performed on the flow visualization pump. PIFV of the lower housing secondary flow path is currently in progress.

## RESULTS AND DISCUSSION

This section will report detailed findings of our analyses for the nominal operating condition: 7 L/min, 4500 rpm. The off-design flow characteristics of the pump will be briefly summarized.

### H-Q performance

Our CFD analyses were initially validated by computing the pressure head (H) vs. flow (Q) performance of the pump. If the CFD predictions significantly differ from experiment in this area, then detailed analysis of internal flow structures has questionable value. Table 1 compares the measured vs. computed values. The CFD predictions are within 10% of the experimental values. This slight underprediction of pressure is consistent with our past experiences in blood pump analysis.

### Overall pump flow patterns

Figure 3 shows several planar cuts through the pump to represent overall pump behavior. As expected, pressure head is generated in the impeller blading, and dynamic pressure is converted to static pressure in the volute and exit channel. Pressure gradients in the secondary flow paths were determined to derive from pressure bleed effects from the higher pressure volute and not from centrifugal viscous pumping. Examination of the velocity magnitude field indicates: (1) a slight flow deficit in the inlet elbow, (2) a slow flow region in the rotor's central core, especially at the lower housing floor, and (3) relatively high velocities in the lower housing secondary flow path, which indicates good surface washing occurs there.

### Inlet channel flow patterns

Head-to-head comparison of the CFD and experimental analyses of flows in the inlet channel is shown in Fig. 4. Very good agreement is observed between the two methods of analysis. Note the slight geometric differences between the CFD geometry

**TABLE 1.** Measured vs. predicted pressure head (H) for three cases of flow (Q) and speed ( $\omega$ )

Q (L/min)	$\omega$ (rpm)	$H_{\text{exp}}$ (mm Hg)	$H_{\text{CFD}}$ (mm Hg)
3	3500	80	73
7	4500	135	122
10	5200	150	145

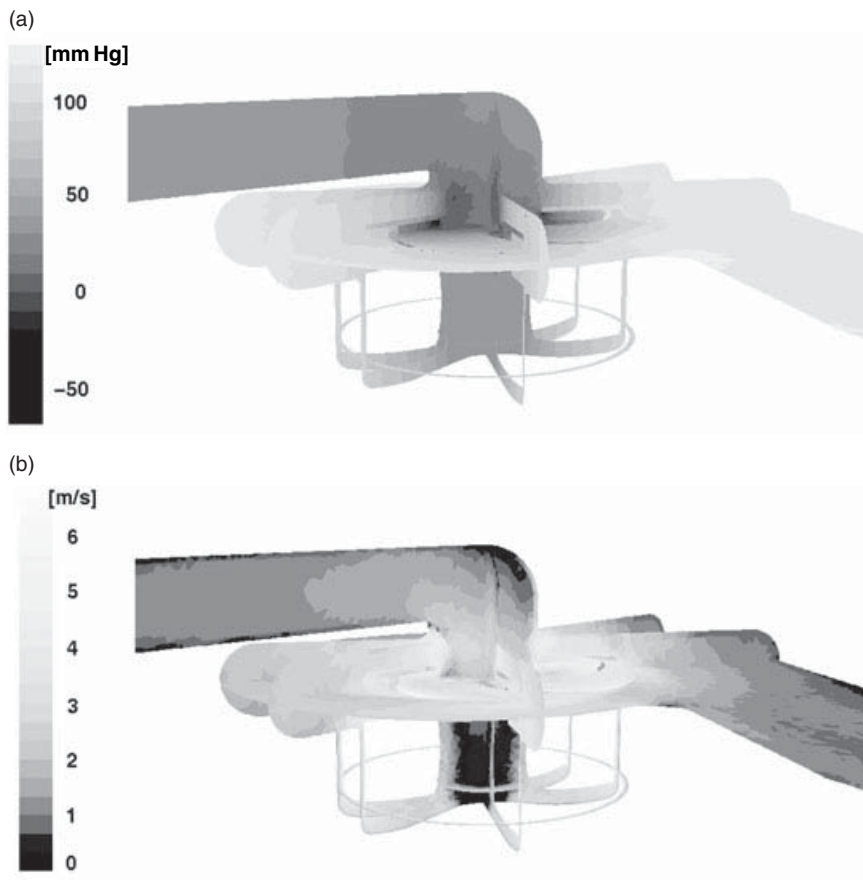


**FIG. 3.** Multiple planar cuts through entire pump geometry: (a) static pressure; (b) velocity magnitude.

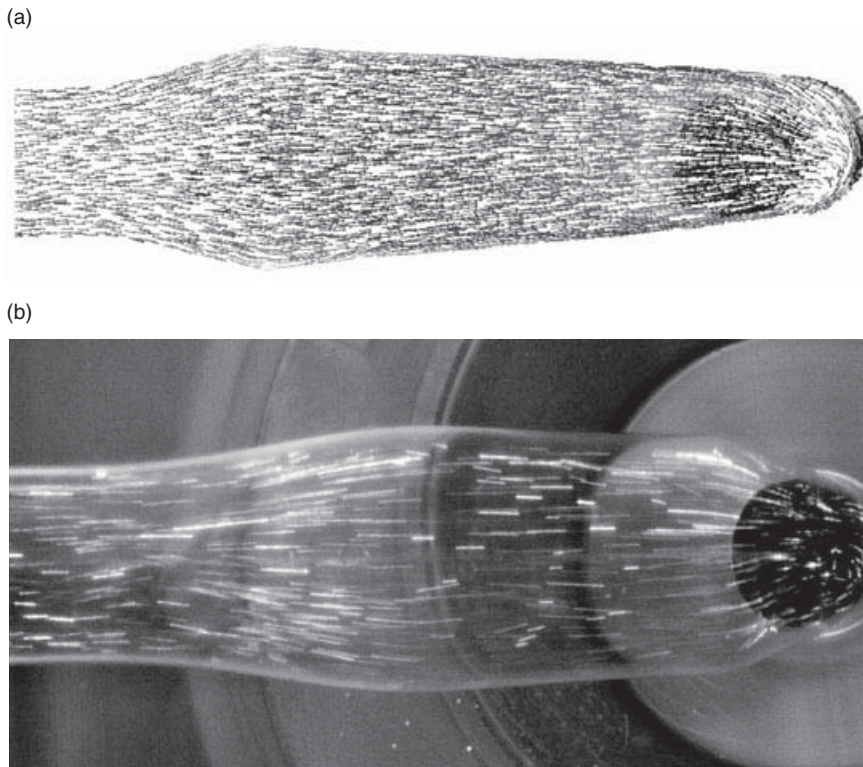


**FIG. 4.** Flows at pump inlet: (a) computational fluid dynamics (CFD) prediction; (b) experimental flow visualization.

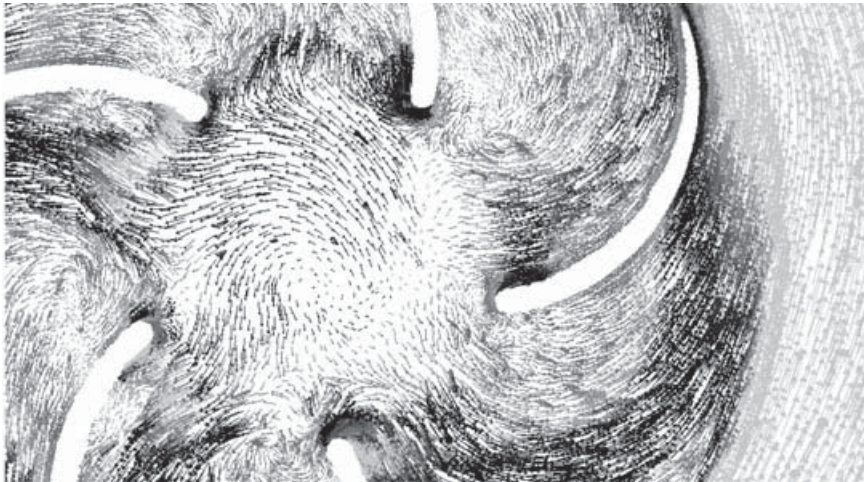


FIG. 5. Midplane cut through impeller blading.

and the flow visualization geometry. These differences reflect slight ergonomic design changes that do not significantly impact the fluid dynamics of the pump. Overall the inlet flow is well behaved and clean. Careful examination reveals a slight degree of swirling flow in the elbow. CFD analysis indicates that a small pocket of preswirl is induced from the impeller and migrates upward into the elbow. The pocket is contained in size and extent by the main flow entering the rotor central core. No flow stasis is observed related to this swirling flow structure. In fact, vigorous surface washing is associated with the preswirl pocket.

#### Impeller blading flow patterns

For this study, CFD analysis was our only option for investigating flow behavior in the impeller blading. Flow visualization was prohibited there because the rotor was fabricated from titanium and electromagnetic components obstructed the view. Figure 5 indicates that the flow enters the blading at a very poor angle of incidence. This misalignment derives from the necessity of the flow to turn 90 degrees, mechanically unassisted, to enter the blade passage. However, one can clearly see that, once inside the blade-to-blade passage, the flow quickly reorganizes and exits the blading well attached and well guided. No in vivo thrombus problems have been associated with the blading leading edges.

#### Rotor central core flow patterns

Flow from the inlet channel passes through the central opening of the impeller shroud and plunges into the central core of the rotor. Figure 6 indicates that most of the flow diverts 90 degrees into the impeller blade passages and a smaller portion of the flow convects deeply in the central core. One might

expect to find a relatively quiescent, stagnant flow zone near the lower housing floor. However, details of the CFD analysis indicate otherwise, revealing the central core contains quite complex three-dimensional flow structures. First, there exists a centralized, strongly vortical structure that precesses unsteadily (like a tornado) and provides a wandering pattern of surface washing of the lower housing floor. Second, flow recirculates or leaks through the lower housing secondary flow path, driven by the higher volute pressure toward the lower central core pressure (see Fig. 3a). This leakage flow rejoins the main flow path (i.e., the blade passage flow) by migrating up the interior walls of the central core, hence providing some degree of surface washing there. Finally, note that a large recirculation of flow is predicted in

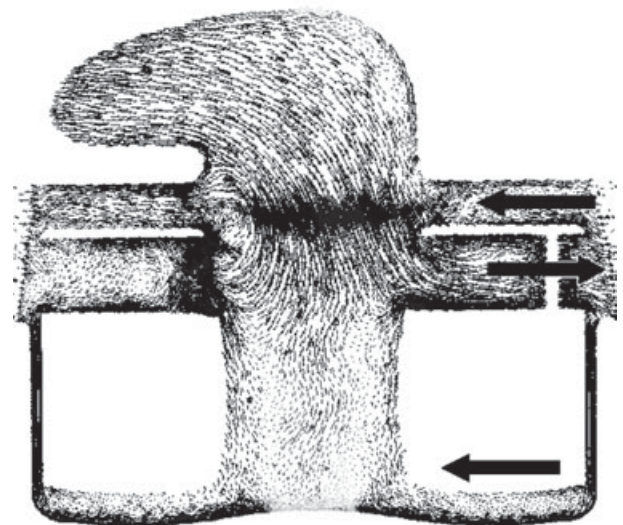
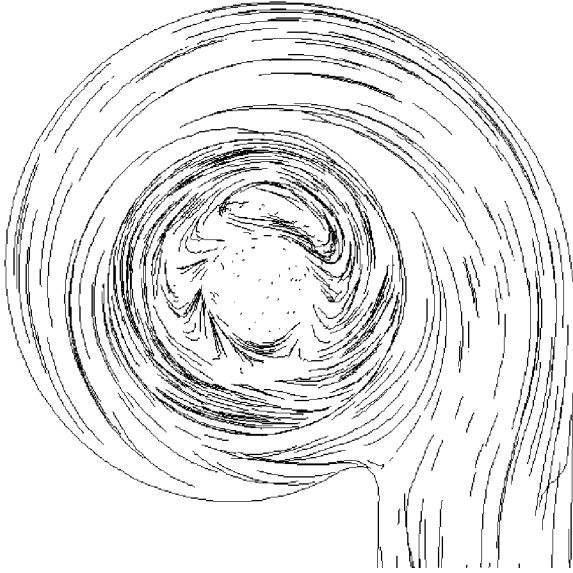


FIG. 6. Planar cut through middle of pump. Arrows indicate local flow directions.

(a)



(b)



**FIG. 7.** Flows in volute above the impeller shroud: (a) computational fluid dynamics (CFD) prediction; (b) experimental flow visualization.

the upper housing secondary flow path in which the fluid moves in the reverse direction of the impeller passage flow.

#### **Volute flow patterns**

Flow in the volute is found to be well behaved. Figure 7 confirms that reverse flow occurs in the

upper housing secondary flow path, indicated by the inwardly spiraling streaklines. The CFD prediction agrees fairly well, but also shows a localized transient recirculatory flow feature.

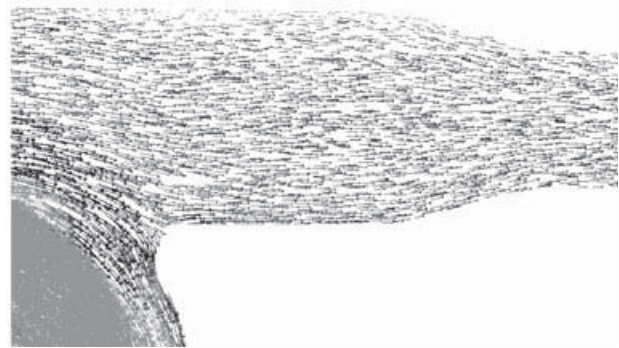
#### **Outlet channel flow patterns**

Flow in the outlet channel is well behaved (Fig. 8). As expected, the cutwater has a flow stagnation point. It was found that the location of the stagnation point depends on the pump volumetric flow rate. Downstream of the cutwater is a small region of disturbed flow that immediately clears as pump flow rate increases.

#### **Off-design flow behavior**

Computational fluid dynamic analyses were performed for low (3 L/min, 3500 rpm) and high (10 L/min, 5200 rpm) operating conditions. Flow visualization was performed for 12 discretely differ-

(a)



(b)

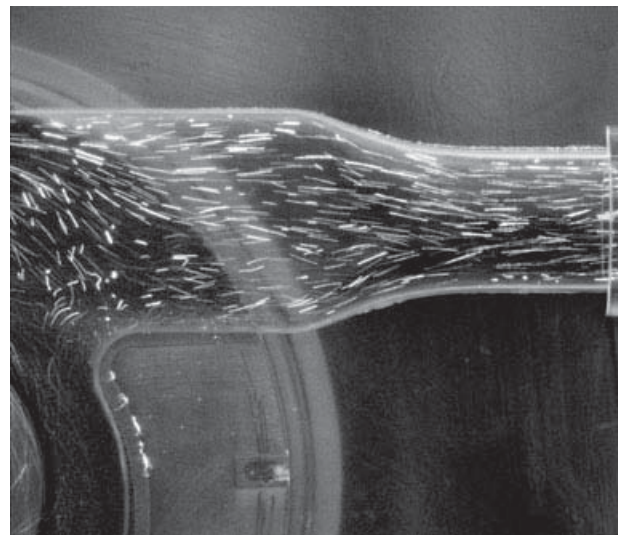


**FIG. 8.** Flows at pump outlet: (a) computational fluid dynamics (CFD) prediction; (b) experimental flow visualization.

ent flow conditions spanning the low and high operating points. PIFV was also performed for a case having continuously variable flow rates from 0 to 12 L/min. Overall, we discovered that the HeartMate III has remarkably clean fluid dynamics over the entire range of operating conditions. The slight flow irregularities indicated by CFD, flow visualization, and PIFV become more exaggerated in their strength and size at lower flow rates. However, these flow behaviors quickly mitigate and vanish at higher flow rates. It should be noted that no in vivo thrombus problems have been observed for pump flows roughly corresponding to either the normal flow ( $4.8 \pm 1.4$  L/min,  $n = 11$ , 54-day average study duration) or the low flow ( $3.2 \pm 0.9$  L/min,  $n = 4$ , 42-day average study duration) operating conditions.

### CONCLUSIONS

Comparison of CFD predictions to experimental imaging shows good agreement. Both CFD and experimental PIFV confirmed well-behaved flow fields in the main components of the HeartMate III

pump: inlet, volute, and outlet. The pump evidences remarkably little flow stasis across all flow conditions. CFD predicted excellent washing of the rotor inlet and rotor cavity by virtue of pressure-driven backflows in the rotor-housing gaps and an unsteady vortex within the centrally open rotor. The findings are consistent with clean pumps explanted from an extensive series of chronic in vivo studies. Despite volumetric and viscous losses, the pump hydrodynamic efficiency approaches 30% at the design point (135 mm Hg, 7 L/min, 4500 rpm). The unique design of the HeartMate III produces an effective collaboration of three separate flow paths to result in a pump having clean flow features, low thrombogenicity, and adequate hydraulic efficiency across its entire operating range.

### REFERENCES

1. Bourque K, Gernes DB, Loree HM 2<sup>nd</sup>, et al. HeartMate III: pump design for a centrifugal LVAD with a magnetically levitated rotor. *ASAIO J* 2001;47:401–5.
2. Loree HM, Bourque K, Gernes DB, et al. HeartMate III: design and in vivo studies of a maglev centrifugal LVAD. *Artif Organs* 2001;25:386–91.